Contribution from the School of Chemical Sciences, University of Illinois, Urbana, Illinois 61801, and the Department of Chemistry, University of Colorado, Boulder, Colorado 80309

Magnetic Exchange Interactions in Binuclear Transition-Metal Complexes. 18. Dianions of 5,8-Dihydroxy-1,4-naphthoquinone, 1,4-Dihydroxy-9,10-anthraquinone, and 1,5-Dihydroxy-9,10-anthraquinone as Bridging Ligands in Copper(II) and Nickel(II) Complexes[1]

CORTLANDT G. PIERPONT,*[2] LYNN C. FRANCESCONI,[3] and DAVID N. HENDRICKSON*[3,4]

Received May 4, 1978

The structure of $[Cu_2(dien)_2(DHNQ)](BPh_4)_2$, where $DHNQ^{2-}$ is the dianion of 5,8-dihydroxy-1,4-naphthoquinone and dien is diethylenetriamine, has been determined using heavy-atom, X-ray methods. The compound crystallizes in the monoclinic space group $P2_1/n$ with two formula weights in a unit cell of dimensions a = 15.505 (4) Å, b = 17.700 (4) Å, c = 10.533 (3) Å, β = 92.56 (2)°, d(calcd) = 1.34 g cm^{-3}, and d(exptl) = 1.33 (1) g cm^{-3}. The structure was refined to conventional discrepancy factors of R = 0.069 and R_w = 0.084 for 2818 observed reflections. The compound is a BPh_4^- salt of a centrosymmetric binuclear copper(II) complex, $[Cu_2(dien)_2(DHNQ)]^{2+}$. The molecular dimensions of the planar $DHNQ^{2-}$ moiety are nearly identical with those previously reported for uncomplexed 5,8-dihydroxy-1,4-naphthoquinone. The coordination geometry about the copper(II) ions is intermediate between square pyramidal (SP) and trigonal bipyramidal (TBP). The Q-band EPR spectrum of this complex clearly points to the SP choice, which places one primary nitrogen of the dien ligand in the apical site of the distorted SP geometry. This is unusual for dien. The Cu–Cu distance in this binuclear complex is 8.075 (3) Å. The preparations of several other binuclear copper(II) and nickel(II) complexes bridged by $DHNQ^{2-}$, $QUIN^{2-}$ (dianion of 1,4-dihydroxy-9,10-anthraquinone), and $DHAQ^{2-}$ (1,5-dihydroxy-9,10-anthraquinone) are reported. Variable-temperature (ca. 4.2–220 K) magnetic susceptibility data are reported for $[Ni_2(tren)_2(DHNQ)](BPh_4)_2$, $[Ni_2(tren)_2(QUIN)](BPh_4)_2$, and six copper(II) compounds variously bridged by $DHNQ^{2-}$, $QUIN^{2-}$, and $DHAQ^{2-}$ and having different triamine nonbridging ligands. None of the compounds shows evidence of a magnetic exchange interaction in the magnetism data. Copper hyperfine is seen in the EPR spectrum for only one compound, $[Cu_2(dien)_2(DHNQ)](BPh_4)_2$. The eight-line hyperfine (average spacing 84 G) seen on the $g_\parallel$ signal for this compound demonstrates that there is a weak magnetic exchange ($|J|$ > ca. 0.02 cm^{-1}) present in this compound. CNDO/2 molecular orbital calculations on $DHNQ^{2-}$ are used to explain qualitatively why there is no appreciable antiferromagnetic interaction propagated by $DHNQ^{2-}$, whereas such interactions have been seen for complexes bridged by the dianion of 2,5-dihydroxy-1,4-benzoquinone.

Introduction

Various hydroxyquinones are present in pigments[5] and also in humic substances.[6] Complexes of lawsone (2-hydroxy-1,4-naphthoquinone) with Fe(II), Fe(III), and Pd(II) have recently been studied.[7-9] It was found that Fe(III) promotes the dimerization of lawsone.[7] In another recent study,[10] the properties of rare-earth chelates of hydroxynaphthoquinone antibacterials were described.

In a previous paper[11] in this series, the preparation and characterization of several binuclear nickel(II) and copper(II) complexes bridged by the dianions of 2,5-dihydroxy-1,4-benzoquinone and chloranilic acid were reported. Antiferromagnetic exchange interactions were detected for several of these binuclear complexes. It was of considerable interest to find that the antiferromagnetic interaction in $[Ni_2(tren)_2(DHBQ)](BPh_4)_2$, where tren is 2,2′,2″-triaminotriethylamine and $DHBQ^{2-}$ is the dianion of 2,5-dihydroxy-1,4-benzoquinone, is greater than the interaction reported[12] for the analogous squarate ($C_4O_4^{2-}$)-bridged complex. In the series of compounds with the composition $[Ni_2(tren)_2(bridge)](BPh_4)_2$, the antiferromagnetic exchange interaction ($\mathbf{H} = 2J\mathbf{S}_1\cdot\mathbf{S}_2$) varies in the following order: oxalate (J = −15.6 cm^{-1}), followed by $DHBQ^{2-}$ (J = −1.1 cm^{-1}), the weakest being found for the squarate (J = −0.4 cm^{-1}). The bridging units in these octahedral Ni(II) complexes are illustrated.

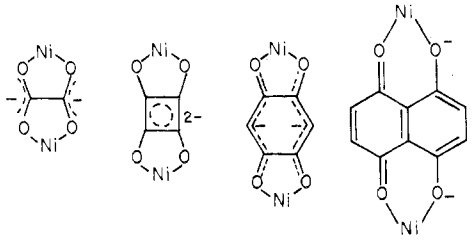

Thus, it is clear that the interaction does not simply decrease as the Ni–Ni distance increases but varies in response to the availability of bridge molecular orbitals of the correct symmetry to propagate an interaction between the metal orbitals in which the unpaired electrons reside. Additional analogous dianionic bridging moieties were sought to add to the series; bridges with even greater extension were of particular interest. In this paper, we report the preparation and characterization of several binuclear copper(II) and nickel(II) complexes bridged by the dianions of 5,8-dihydroxy-1,4-naphthoquinone (commonly known as naphthazarin), 1,4-dihydroxy-9,10-anthraquinone (quinizarin), and 1,5-dihydroxy-9,10-anthraquinone. The crystal structure of $[Cu_2(dien)_2(DHNQ)](BPh_4)_2$, where dien is diethylenediamine and $DHNQ^{2-}$ is the dianion of 5,8-dihydroxy-1,4-naphthoquinone, is also reported.

Experimental Section

Compound Preparation. The tridentate ligands diethylenetriamine (Union Carbide), dipropylenetriamine (Aldrich), 1,1,4,7,7-pentamethyldiethylenetriamine (Ames Laboratories, Inc.) and 2,2′,2″-triaminotriethylamine (Ames) were used as received. Quinizarin (1,4-dihydroxy-9,10-anthraquinone) and 1,5-dihydroxy-9,10-anthraquinone were purchased from Eastman. All elemental analyses were performed in the microanalytical laboratory of the School of Chemical Sciences. The analytical data for all compounds are given in Table I.[13]

The ligand 5,8-dihydroxy-1,4-naphthoquinone was prepared by a slight modification of the method of Kuroda.[14] Some 12 g of 1,5-dinitronaphthalene was suspended in ca. 50 mL of concentrated H_2SO_4. A suspension of 12 g of elemental sulfur in 90 mL of 15–18% fuming sulfuric acid was added slowly so as to maintain the temperature at a value lower than 60 °C. The suspension was stirred for ca. 1.5 h at 60° and then it was poured onto some 420 g of ice. The resulting solution was filtered through a porcelain Büchner filter to remove the unreacted 1,5-dinitronaphthalene and sulfur. The dark blue filtrate was then digested on a steam bath for a few hours until a dark red precipitate formed. The precipitate was filtered, washed several times with H_2O and then diethyl ether, and finally dried in vacuo over P_4O_{10}. Sublimation of the powder resulted in dark green crystalline product.

0020-1669/78/1317-3470$01.00/0

Samples of **$[Cu_2(dien)_2(DHNQ)](BPh_4)_2$**, **$[Cu_2(dien)_2(DHAQ)](BPh_4)_2$**, **$[Cu_2(dpt)_2(DHAQ)](BPh_4)_2$**, **$[Ni_2(tren)_2(DHNQ)](BPh_4)_2$**, and **$[Ni_2(tren)_2(QUIN)](BPh_4)_2$**, where dien is diethylenetriamine, dpt is dipropylenetriamine, tren is 2,2′,2″-triaminotriethylamine, $DHNQ^{2-}$ is the dianion of 5,8-dihydroxy-1,4-naphthoquinone, $DHAQ^{2-}$ is the dianion of 1,5-dihydroxy-9,10-anthraquinone, and $QUIN^{2-}$ is the dianion of 1,4-dihydroxy-9,10-anthraquinone, were prepared in a similar fashion as the technique used to prepare binuclear copper(II) and nickel(II) complexes of 2,5-dihydroxy-1,4-benzoquinone and chloranilic acid.[11] The details of a typical preparation of $[Cu_2(dien)_2(DHNQ)](BPh_4)_2$ are given. Some ca. 0.5 g (2 mmol) of $CuSO_4 \cdot 5H_2O$ was dissolved in ca. 100 mL of H_2O followed by the addition of ca. 0.2 mL (2 mmol) of dien. Approximately 100 mL of basic H_2O solution containing ca. 0.2 g (1 mmol) of DHNQ was added to the first solution. The resulting solution was filtered through a fine-porosity frit. To the filtrate, a filtered aqueous solution of $NaBPh_4$ was added to give a dark blue precipitate which was vacuum filtered and washed several times with H_2O followed by several washings with diethyl ether. The solid was dried in vacuo over P_4O_{10}.

Because quinizarin and 5,8-dihydroxy-1,4-naphthoquinone readily form polymeric metal–quinone complexes,[15-17] it was necessary to prepare **$[Cu_2(Me_5dien)_2(DHNQ)](BPh_4)_2$**, **$[Cu_2(dpt)_2(DHNQ)](BPh_4)_2$**, **$[Cu_2(dien)_2(QUIN)](BPh_4)_2$**, **$[Cu_2(Me_5dien)_2(QUIN)](BPh_4)_2$**, and **$[Cu_2(dpt)_2(QUIN)](BPh_4)_2$** starting from a copper quinone polymer. The compound **$[Cu_2(dpt)_2(DHAQ)](BPh_4)_2$** may also be prepared from a sample of the Cu–DHAQ polymer; the analytical, IR, and EPR data are the same for samples of this compound as they are obtained from either the above method or the polymer method. The polymer method is exemplified by the preparation details for $[Cu_2(dpt)_2(QUIN)](BPh_4)_2$. Approximately 0.6 g (2.4 mmol) of $CuSO_4 \cdot 5H_2O$ was dissolved in ca. 100 mL of H_2O, and ca. 0.35 mL (2.4 mmol) of dpt was added. Addition of ca. 200 mL of a basic H_2O solution containing 0.3 g (1.2 mmol) of quinizarin led to an immediate precipitation of the polymer $Cu(QUIN) \cdot xH_2O$. This polymer is vacuum filtered onto a fine-porosity frit containing Celite. After the drying on the frit for a few minutes, the polymer and the Celite were suspended in ca. 100 mL of methanol containing 0.32 g (1.3 mmol) of $CuSO_4 \cdot 5H_2O$ and 0.4 mL (3.0 mmol) of dpt. After the mixture was stirred for ca. 3 h, the Cu–QUIN polymer dissolved and the solution was filtered through a fine-porosity frit into a stirred methanol solution of $NaBPh_4$. A dark blue precipitate formed and was vacuum filtered, washed with H_2O and then diethyl ether, and dried in vacuo over P_4O_{10}.

A variation of the above "polymer method" was also found to be useful. In this case, the copper quinone polymer was first isolated by the methods of Bottlei[16] or Holtzclaw[15] and then the polymer was suspended in methanol into which a stoichiometric amount of the appropriate triamine was added. After the suspension was stirred for 4–12 h, stoichiometric amounts of $Cu(NO_3)_2 \cdot 3H_2O$ and the triamine were added. The resulting solution was filtered through a fine-porosity frit. To this vigorously stirred solution was slowly added a filtered methanol solution of $NaBPh_4$. A fine powder formed which was vacuum filtered onto a medium-porosity frit, washed with H_2O and diethyl ether, and dried in vacuo over P_4O_{10}.

Most of the compounds were recrystallized by rapid evaporation of a CH_3CN solution. Well-formed crystals of $[Cu_2(Me(dien))_2(DHNQ)](BPh_4)_2$ and $[Cu_2(dien)_2(DHNQ)](BPh_4)_2$ were obtained by slow evaporation of CH_3CN solutions.

Physical Measurements. Variable-temperature (4.2–240 K) magnetic susceptibilities were measured with a Princeton Applied Research Model 150 A vibrating-sample magnetometer operating at 12.7 kG and calibrated with $CuSO_4 \cdot 5H_2O$ as described in a previous paper.[18]

EPR spectra of powdered samples were recorded on a Varian E-9 X-band spectrometer and a Varian E-15 Q-band spectrometer operating at 9.1–9.5 and 35 GHz, respectively. The X-band frequency was determined using a Hewlett-Packard Model 5240A 12.4-GHz digital frequency meter, while the Q-band frequency was calibrated with DPPH ($g = 2.0036$). X-band spectra were recorded at ca. 300 and ca. 80 K. Q-band spectra were taken at ca. 300 and ca. 110 K.

IR spectra were obtained on a PE Model 467 spectrophotometer. Each sample was prepared as a KBr pellet.

Structure Determination of $[Cu_2(dien)_2(DHNQ)](BPh_4)_2$. A crystal of the copper dihydroxynaphthoquinone complex was mounted and centered on a Syntex $P\bar{1}$ automated diffractometer equipped with a graphite crystal monochromator. Photographs taken on other crystals of the complex indicated monoclinic symmetry with extinction patterns consistent with space group $P2_1/n$. The centered settings of 15 reflections with 2θ values greater than 25° (Mo Kα radiation) were refined by least-squares procedures and used to calculate the cell constants given in Table II. A complete data set was collected within the angular range $2° \leq 2\theta \leq 50°$ by the θ–2θ scan technique. A symmetrical scan range of ±0.6° was used with a scan rate of 4°/min. Four standard reflections monitored after every 96 reflections measured showed only normal variations in intensity. The data were corrected for Lorentz, polarization, and absorption effects. Of the 5754 reflections measured, 2818 independent reflections were found to have $F_o^2 > 3\sigma(F_o^2)$ and were used in the refinement.

Table II. Crystal Data for $[Cu_2(dien)_2(O_4C_{10}H_4)](BPh_4)_2$

formula weight 1077.26	Mo Kα radiation
monoclinic	$\mu = 8.30$ cm^{-1}
space group $P2_1/n$	transmission coeff: max = 0.763; min = 0.725
$a = 15.505$ (4) Å	d(exptl) = 1.33 (1) g/cm^3
$b = 17.700$ (4) Å	d(calcd) = 1.34 g/cm^3
$c = 10.533$ (3) Å	crystal size: 0.43 × 0.39 × 0.31 mm
$\beta = 92.56$ (2)°	
$V = 2887.7$ (12) Å^3	

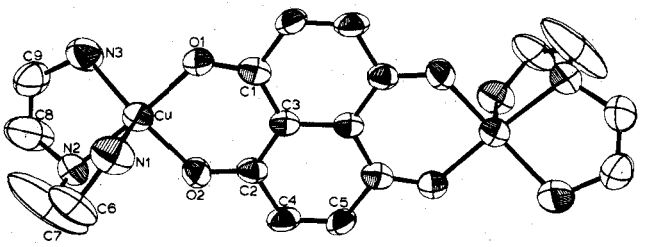

Figure 1. ORTEP plotting of $[Cu_2(dien)_2(DHNQ)]^{2+}$. Hydrogen atoms are not shown.

The Cu atom position was determined from a three-dimensional Patterson map. Least-squares refinement of its positional and isotropic thermal parameters gave discrepancy factors

$$R = (\sum||F_o| - |F_c||)/\sum|F_o| = 0.447$$

$$R_w = [\sum w(|F_o| - |F_c|)^2/wF_o^2]^{1/2} = 0.512$$

where w is the weighting factor defined as $4F_o^2/\sigma^2(F_o^2)$, and F_o and F_c are the observed and calculated structure factors. A difference Fourier map calculated from the Cu refinement revealed the positions of all nonhydrogen atoms of the structure. Cycles of isotropic refinement converged with $R = 0.100$ and $R_w = 0.128$. Three cycles of anisotropic refinement converged with $R = 0.078$ and $R_w = 0.095$. In all calculations the phenyl rings of the anion were treated as rigid groups with a C–C bond length of 1.392 Å. The locations of all hydrogen atoms of the cation were determined from a difference Fourier. Hydrogen positions of the anion were calculated assuming a C–H length of 0.95 Å. Their fixed contributions were included in a final refinement which converged with $R = 0.069$ and $R_w = 0.084$. The error in an observation of unit weight was 2.13. The largest peak on the final difference Fourier map was 0.3 e/Å^3 or about 20% the height of a typical C atom. All major peaks were in the vicinity of the phenyl rings of the anion. Although the thermal parameters of the dien ethylene carbon atoms indicate some disorder, particularly C(7) and C(8), the final difference Fourier showed no significant features in that area. Computer programs, calculational procedures, and sources of scattering factors have been noted previously.[19] Final positional and thermal parameters of atoms and groups are presented in Tables III and IV. A table of the final values of $|F_o|$ and $|F_c|$ is available.

Results and Discussion

Description of the Structure of $[Cu_2(dien)_2(DHNQ)](BPh_4)_2$. The $[Cu_2(dien)_2(DHNQ)]^{2+}$ cation is centered about the origin of the unit cell and is therefore required to be centrosymmetric. A view of the cation alone appears in Figure 1. Figure 2 shows the cation and the two adjacent BPh_4^- anions. Intramolecular dimensions are given in Table V.

The coordination geometry about the Cu centers of the cation is intermediate between the conventional square-py-

Table III. Structural Parameters for $[Cu_2(dien)_2(O_4C_{10}H_4)](BPh_4)_2$

atom[a]	x	y	z	B_{11}[b]	B_{22}	B_{33}	B_{12}	B_{13}	B_{23}
Cu	−0.21316 (6)	0.12730 (6)	0.03984 (9)	4.58 (5)	4.42 (5)	3.98 (5)	0.54 (4)	0.41 (3)	0.54 (4)
O(1)	−0.1549 (3)	0.0536 (3)	0.1423 (5)	5.0 (3)	5.3 (2)	3.7 (2)	1.2 (2)	1.2 (2)	1.2 (2)
O(2)	−0.1254 (3)	0.1236 (3)	−0.0839 (5)	4.8 (3)	4.6 (3)	4.8 (3)	1.3 (2)	1.0 (2)	1.6 (2)
N(1)	−0.3057 (5)	0.0519 (4)	−0.0681 (7)	7.2 (5)	5.5 (3)	5.8 (4)	−0.2 (3)	−0.6 (3)	0.2 (3)
N(2)	−0.2772 (4)	0.2087 (4)	−0.0619 (6)	4.7 (3)	4.9 (3)	4.6 (3)	0.9 (3)	0.0 (3)	0.5 (3)
N(3)	−0.2628 (5)	0.1775 (4)	0.1910 (6)	7.4 (5)	6.3 (4)	4.5 (4)	1.3 (3)	−0.6 (3)	−0.7 (3)
C(1)	−0.0884 (5)	0.0149 (4)	0.1161 (7)	4.4 (4)	3.6 (4)	3.3 (3)	−0.4 (3)	−0.3 (3)	0.1 (3)
C(2)	−0.0614 (5)	0.0776 (4)	−0.0875 (7)	4.5 (4)	3.0 (3)	3.0 (3)	−0.1 (3)	0.2 (3)	0.4 (3)
C(3)	−0.0378 (4)	0.0236 (4)	0.0060 (7)	3.7 (4)	8.4 (10)	3.0 (3)	−0.4 (3)	0.1 (3)	0.1 (3)
C(4)	−0.0079 (6)	0.0848 (7)	−0.1948 (7)	6.7 (4)	3.7 (3)	3.0 (4)	0.3 (3)	1.3 (3)	0.9 (3)
C(5)	0.0621 (5)	0.0422 (4)	−0.2079 (7)	5.1 (5)	4.5 (4)	3.3 (4)	0.6 (3)	1.5 (3)	0.5 (3)
C(6)	−0.3461 (7)	0.0970 (6)	−0.1639 (10)	8.1 (6)	6.2 (5)	6.2 (6)	0.8 (5)	−4.4 (5)	0.5 (4)
C(7)	−0.3382 (13)	0.1785 (6)	−0.1447 (16)	29.5 (20)	3.3 (6)	16.1 (13)	0.6 (9)	−15.2 (14)	1.3 (7)
C(8)	−0.3164 (12)	0.2598 (9)	0.0292 (12)	25.7 (17)	16.8 (14)	4.9 (7)	16.9 (13)	0.3 (8)	−0.2 (7)
C(9)	−0.3169 (7)	0.2411 (5)	0.1495 (10)	7.8 (7)	5.1 (5)	5.5 (5)	1.5 (4)	1.6 (4)	−0.6 (4)
B	−0.1594 (6)	0.3013 (4)	0.5254 (8)	4.3 (4)	2.1 (3)	3.1 (4)	0.2 (3)	0.2 (3)	0.3 (3)

group[c]	x_c	y_c	z_c	ϕ	θ	ρ
R(1)	−0.1444 (2)	0.3720 (2)	0.2586 (3)	0.826 (3)	−2.903 (3)	1.958 (3)
R(2)	−0.3285 (2)	0.3478 (2)	0.6451 (3)	2.276 (5)	2.307 (3)	−2.404 (5)
R(3)	−0.1440 (2)	0.1272 (2)	0.5058 (3)	1.685 (3)	−2.917 (3)	0.088 (3)
R(4)	−0.0182 (2)	0.3652 (2)	0.7086 (3)	2.970 (4)	−2.474 (3)	−0.974 (4)

[a] Estimated standard deviations of the least significant figures are given in parentheses. [b] Anisotropic thermal parameters are in the form $\exp[-0.25(B_{11}a^{*2}h^2 + B_{22}b^{*2}k^2 + B_{33}c^{*2}l^2 + 2B_{12}a^*b^*hk + 2B_{13}a^*c^*hl + 2B_{23}b^*c^*kl)]$ and are in units of Å^2. [c] x_c, y_c, and z_c are the fractional coordinates of the rigid group centers. The angles ϕ, θ, and ρ are in radians and have been defined previously: R. Eisenberg and J. A. Ibers, *Inorg. Chem.*, **4**, 773 (1965).

Table IV. Derived Positional and Isotropic Thermal Parameters for Group Carbon Atoms in $[Cu_2(dien)_2(O_4C_{10}H_4)](BPh_4)_2$

atom	x	y	z	B, Å^2
		R(1)		
C(1)	−0.0931 (3)	0.3104 (2)	0.2944 (5)	4.7 (2)
C(2)	−0.1529 (3)	0.3385 (3)	0.3770 (4)	3.3 (1)
C(3)	−0.2042 (3)	0.4001 (3)	0.3412 (4)	3.6 (1)
C(4)	−0.1957 (3)	0.4336 (2)	0.2229 (4)	4.3 (2)
C(5)	−0.1359 (3)	0.4055 (3)	0.1403 (4)	4.8 (2)
C(6)	−0.0846 (3)	0.3439 (3)	0.1761 (4)	5.5 (2)
		R(2)		
C(1)	−0.2502 (3)	0.3679 (3)	0.7052 (4)	4.8 (2)
C(2)	−0.2513 (2)	0.3289 (3)	0.5905 (4)	3.3 (1)
C(3)	−0.3297 (3)	0.3087 (3)	0.5304 (4)	3.8 (1)
C(4)	−0.4069 (2)	0.3276 (3)	0.5850 (5)	5.1 (2)
C(5)	−0.4057 (3)	0.3666 (3)	0.6997 (5)	5.4 (2)
C(6)	−0.3274 (3)	0.3868 (3)	0.7598 (4)	5.6 (2)
		R(3)		
C(1)	−0.0729 (2)	0.1738 (2)	0.4907 (5)	3.8 (1)
C(2)	−0.1525 (3)	0.2052 (2)	0.5166 (5)	3.5 (1)
C(3)	−0.2236 (2)	0.1586 (3)	0.5317 (5)	4.0 (1)
C(4)	−0.2152 (3)	0.0806 (2)	0.5209 (5)	5.1 (2)
C(5)	−0.1356 (3)	0.0492 (2)	0.4950 (5)	4.9 (2)
C(6)	−0.0645 (2)	0.0958 (3)	0.4799 (5)	4.8 (2)
		R(4)		
C(1)	−0.0366 (3)	0.4017 (3)	0.5936 (4)	4.1 (1)
C(2)	−0.0758 (3)	0.3330 (3)	0.6190 (4)	3.6 (1)
C(3)	−0.0574 (3)	0.2964 (2)	0.7340 (5)	4.2 (1)
C(4)	0.0002 (4)	0.3286 (3)	0.8235 (4)	5.2 (2)
C(5)	0.0394 (3)	0.3973 (3)	0.7981 (4)	5.2 (2)
C(6)	0.0210 (3)	0.4339 (2)	0.6832 (5)	4.8 (2)

Table V. Principal Intramolecular Bonding Parameters for the $[Cu_2(dien)_2(O_4C_{10}H_4)]^{+2}$ Cation

Distances, Å

Cu-O(1)	1.896 (5)	C(2)-C(4)	1.437 (10)
Cu-O(2)	1.927 (5)	C(3)-C(3)′	1.450 (14)
Cu-N(1)	2.233 (8)	C(4)-C(5)	1.333 (10)
Cu-N(2)	2.028 (6)	N(1)-C(6)	1.412 (11)
Cu-N(3)	2.007 (7)	C(6)-C(7)	1.460 (15)
O(1)-C(1)	1.278 (8)	N(2)-C(7)	1.367 (14)
O(2)-C(2)	1.286 (8)	N(2)-C(8)	1.470 (13)
C(1)-C(3)	1.438 (10)	C(8)-C(9)	1.310 (14)
C(1)-C(5)′	1.446 (10)	N(3)-C(9)	1.460 (11)
C(2)-C(3)	1.409 (10)		

Angles, Deg

O(1)-Cu-O(2)	91.7 (2)	C(3)-C(1)-C(5)′	117.8 (7)
O(1)-Cu-N(1)	99.1 (2)	C(3)-C(2)-C(4)	118.0 (7)
O(1)-Cu-N(2)	177.2 (2)	C(1)-C(3)-C(2)	120.2 (7)
O(1)-Cu-N(3)	92.4 (2)	C(1)-C(3)-C(3)′	118.8 (8)
O(2)-Cu-N(1)	95.3 (2)	C(2)-C(3)-C(3)′	121.0 (8)
O(2)-Cu-N(2)	90.6 (2)	C(1)-C(5)-C(4)′	122.2 (7)
O(2)-Cu-N(3)	149.2 (3)	C(2)-C(4)-C(5)	122.1 (7)
N(1)-Cu-N(2)	82.4 (3)	Cu-N(1)-C(6)	106.3 (6)
N(1)-Cu-N(3)	114.1 (3)	N(1)-C(6)-C(7)	115.3 (9)
N(2)-Cu-N(3)	84.8 (3)	C(6)-C(7)-N(2)	121.7 (10)
Cu-O(1)-C(1)	127.9 (5)	C(7)-N(2)-C(8)	111.2 (12)
Cu-O(2)-C(2)	127.6 (5)	Cu-N(2)-C(7)	111.6 (6)
O(1)-C(1)-C(3)	126.3 (7)	Cu-N(2)-C(8)	107.4 (6)
O(2)-C(2)-C(3)	125.8 (7)	N(2)-C(8)-C(9)	119.8 (10)
O(1)-C(1)-C(5)′	115.9 (7)	C(8)-C(9)-N(3)	117.1 (9)
O(2)-C(2)-C(4)	116.1 (7)	Cu-N(3)-C(9)	109.9 (5)

Table VI. Deviations from the DHNQ Least-Squares Plane

plane:[a] $8.54x + 11.98y + 4.87z = 0.01$

atom	distance, Å	atom	distance, Å
O(1)	0.013 (6)	C(4)	0.000 (9)
O(2)	0.002 (6)	C(5)	0.023 (9)
C(1)	−0.009 (8)	Cu	−0.101
C(2)	−0.021 (7)	N(2)	−0.169
C(3)	−0.010 (7)	N(3)	0.813

[a] Least-squares plane is in crystal coordinates as defined by W. C. Hamilton, *Acta Crystallogr.*, **18**, 502 (1965).

ramidal (SP) and trigonal-bipyramidal (TBP) five-coordinate polyhedra; see Figure 3. Ligand atoms O(1) and N(2) have a trans bond angle of 177.2 (2)° and may be viewed to occupy axial sites of a trigonal bipyramid or basal sites of a square pyramid. The three bond angles which would describe the equatorial plane of a TBP, N(1)–Cu–O(2), N(1)–Cu–N(3), and O(2)–Cu–N(3), have values of 95.3 (2), 114.1 (3), and 149.2 (3)°, respectively. These values, particularly those including O(2), indicate a distortion toward a SP with N(1) occupying the apical position. Bond lengths to apical donor ligands in SP Cu^{2+} complexes are generally longer than basal values. Consequently, the Cu–N(1) length has a value of 2.233 (8) Å, while values to N(2) and N(3) are 2.028 (6) and 2.007 (7) Å. Structural work has been carried out on three related bridged binuclear Cu^{2+} complexes with dien or substituted dien

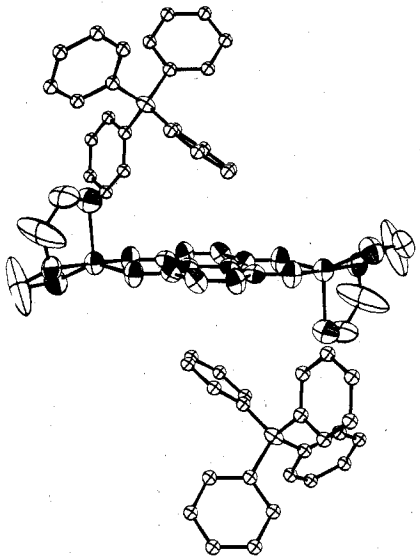

Figure 2. ORTEP plotting of $[Cu_2(dien)_2(DHNQ)]^{2+}$ showing the possible contacts with two BPh_4^- ions.

ligands. Two of these complexes have oxalate bridges; the third has a chloranilate bridge (CA). In each of these cations, as in the present case, there is a clear axial orientation for one oxygen and one nitrogen donor with a bond angle close to 180°. They differ from $[Cu_2(dien)_2(DHNQ)]^{2+}$ in that the second oxygen of the bridging ligand resides in a quasiapical position and has a significantly longer Cu–O length than the axial oxygen. The distribution of the three remaining ligands in the plane normal to the N–Cu–O axis ranges from near SP[20] in $[Cu_2(dien)_2(C_2O_4)]^{2+}$ to near TBP[18] in $[Cu_2(Et_5dien)_2(C_2O_4)]^{2+}$. The $[Cu_2(Me_5dien)_2(CA)]^{2+}$ cation has an intermediate structure (CA^{2-} is the dianion of chloranilic acid).[11] The distortion from SP to TBP within this series appears related to the steric requirements of the dien substituents. Both Cu–O lengths in the present structure are shorter than values found in the other three complex cations. This may be related to a preference of Cu^{2+} for a six-membered chelate ring. The values found are within the range of values (1.90–1.91 Å) normally found for β-diketonate ligands, while oxalate complexes of Cu^{2+} normally have values greater than 1.96 Å. The O–Cu–O bond angle in $[Cu_2(dien)_2(DHNQ)]^{2+}$ is 91.7 (2)° while values found for five-membered chelate rings are near 80°.

Of the three related structures $[Cu_2(Me_5dien)_2(CA)]^{2+}$ most closely resembles $[Cu_2(dien)_2(DHNQ)]^{2+}$. Bond angles in the equatorial plane of the chloranilate-bridged dimer are roughly comparable to those found in the DHNQ dimer with values of 102.1 (2), 106.0 (2), and 151.8 (2)°. However, with an oxygen donor in the apical position, the plane of the quinone bridge of the chloranilate cation is normal to the basal plane of the complex. For the $[Cu_2(dien)_2(DHNQ)]^{2+}$ cation the DHNQ ligand is bound at two basal sites (Figure 3). In both structures the difference between apical and basal bond lengths is approximately 0.2 Å. Structurally, the DHNQ ligand is nearly identical with the uncomplexed dihydroxyquinone.[21] The C–O lengths found in the complex are 1.278 (8) and 1.286 (8) Å compared with 1.30 Å for the free molecule, while in both structures the C–C bonds at the 2–3 and 6–7 positions are the shortest of the ring bonds with values of 1.33 (1) Å for the complex and 1.35 Å for the free quinone.

The diacetate of 5,8-dihydroxy-1,4-naphthoquinone has recently been structurally characterized.[22] The molecular dimensions of the diacetate are similar to those for the $DHNQ^{2-}$ bridge in $[Cu_2(dien)_2(DHNQ)](BPh_4)_2$.

Previous work[23] from these laboratories has shown that down to 4.2 K oxalate-bridged $[Cu_2(dien)_2(C_2O_4)](ClO_4)_2$ does not exhibit any signs of a magnetic exchange interaction. It was further found that metathesis to give the tetraphenylborate $[Cu_2(dien)_2(C_2O_4)](BPh_4)_2$ resulted in a compound that does show an antiferromagnetic exchange interaction with $J = -7.3$ cm^{-1}. It was suggested that the metathesis affected the structure of the binuclear cation such that the cation in the BPh_4^- salt possessed a structure wherein two oxygen atoms were located in the plane of the copper SP coordination geometry. Such a limiting structure where the oxalate bridge is coplanar with the planes of both copper SP would be expected to exhibit a relatively strong antiferromagnetic interaction. In short, the structure suggested for the cation in $[Cu_2(dien)_2(C_2O_4)](BPh_4)_2$ approximates to the unusual structure found in this study for the cation in $[Cu_2(dien)_2(DHNQ)](BPh_4)_2$.

It seems clear from the array of different structures encountered over the series of bridged copper(II) structures that the coordination geometry about the quasi-equatorial plane of the complex is fairly amorphous. The difference in structure about the Cu centers in $[Cu_2(dien)_2(DHNQ)]^{2+}$ and $[Cu_2(dien)_2(C_2O_4)]^{2+}$ is somewhat perplexing but may be related to cation–anion interactions in the case of the DHNQ structure. We have noted previously a strong tendency among complexes with quinone ligands toward formation of π complexes with other unsaturated molecules, particularly benzene. In other structures containing the BPh_4^- anion the cation and anions are well separated but in the present structure one ring of each of the two BPh_4^- anions is located on either side of the DHNQ ligand and pointed toward the carbonyl region. The closest interatomic separations between the cation and anions are 3.39–3.41 Å, indicating no substantial interaction, but the presence of the anions at these positions may influence the coordination geometry about the metal centers. Beyond a possible cation–anion interaction and the ill-defined effects of the larger chelate ring, it is not clear what factors are responsible for the difference in coordination geometry.

Infrared Spectroscopy. A recent study[15] of polymeric copper(II) complexes of $DHNQ^{2-}$, $QUIN^{2-}$, and $DHAQ^{2-}$ and other studies[16,17] of various metal–dihydroxyquinone polymeric complexes have shown that the carbonyl stretching frequency for the uncomplexed dihydroxyquinone shifts ca. 80 cm^{-1} to lower energy upon coordination as a dianion to the metal ions

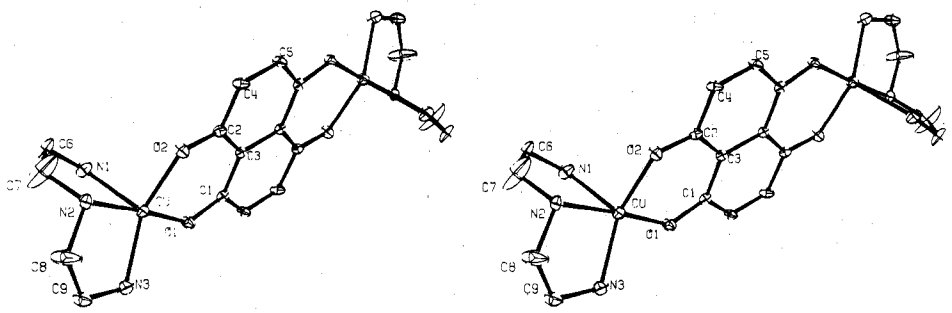

Figure 3. Stereoscopic view of $[Cu_2(dien)_2(DHNQ)]^{2+}$. Hydrogen atoms are not shown.

Table XV. Q-Band EPR g Values

$[Cu_2(dien)_2(DHNQ)](BPh_4)_2$	2.032
	2.096
	2.251[a]
$[Cu_2(Me_5dien)_2(DHNQ)](BPh_4)_2$	2.024
	2.146
	2.213
$[Cu_2(dpt)_2(DHNQ)](BPh_4)_2$	2.015
	2.150
	2.229
$[Cu_2(dien)_2(QUIN)](BPh_4)_2$	2.050
	2.083
	2.261
$[Cu_2(Me_5dien)_2(QUIN)](BPh_4)_2$	2.031
	2.089
	2.217
$[Cu_2(dpt)_2(QUIN)](BPh_4)_2$	2.021
	2.146
	2.225
$[Cu_2(dien)_2(DHAQ)](BPh_4)_2$	2.055
	2.259
$[Cu_2(dpt)_2(DHAQ)](BPh_4)_2$	2.067
	2.204

[a] $A_{\parallel av} = 84$ G.

in the polymer. In all of the binuclear complexes of copper(II) and nickel(II) in this study, a shift of ca. 60 cm^{-1} in the carbonyl stretching frequency to lower energies was observed. This is an indication that the carbonyl oxygen of the quinone is bonding to the metal ion. Three bridging configurations are present in these complexes.

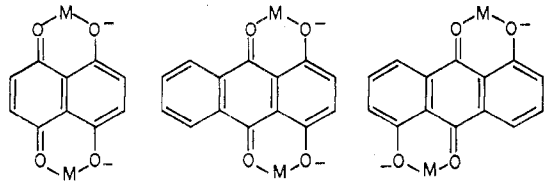

Magnetic Susceptibility. Variable-temperature (ca. 4.2–220 K) magnetic susceptibility data were collected for $[Ni_2(tren)_2(DHNQ)](BPh_4)_2$, $[Cu_2(dien)_2(DHNQ)](BPh_4)_2$, $[Cu_2(Me_5dien)_2(DHNQ)](BPh_4)_2$, $[Cu_2(dpt)_2(DHNQ)](BPh_4)_2$, $[Cu_2(dien)_2(DHAQ)](BPh_4)_2$, $[Cu_2(dpt)_2(DHAQ)](BPh_4)_2$, $[Ni_2(tren)_2(QUIN)](BPh_4)_2$, and $[Cu_2(Me_5dien)_2(QUIN)](BPh_4)_2$. The data are given in Tables VII–XIV.[13] For each complex, there is no evidence of a magnetic exchange interaction down to a temperature of ca. 4.2 K. The effective magnetic moment for each compound is relatively constant and above the spin-only value for either copper(II) or nickel(II). In the case of the binuclear copper(II) complexes this means that the absolute value of the magnetic exchange parameter, J, in the spin Hamiltonian, $-2J\mathbf{S}_1\cdot\mathbf{S}_2$, is less than ca. 0.5 cm^{-1}, whereas $|J|$ for the two binuclear nickel(II) complexes is less than ca. 0.05 cm^{-1}.

EPR Spectroscopy. Copper(II) complexes are particularly amenable to an examination with EPR. Two types of information can be obtained. On the one hand, the pattern of g values seen for a particular complex indicates the coordination geometry about the copper(II) ion. In the case of binuclear complexes, it is possible to identify spectral features that are characteristic of the presence of a magnetic exchange interaction. The copper(II) binuclear complexes in this study were prepared as BPh_4^- salts in order to maximize the opportunity of seeing copper hyperfine splitting, which can be used simply to tell whether a magnetic exchange interaction is present. Other EPR features that point to such an interaction include the "half-field" $\Delta M_s = 2$ transition and the rarely seen[11,24] singlet-to-triplet transitions.

The eight binuclear copper(II) complexes prepared in this study were examined by EPR spectroscopy at both X- and Q-band frequencies. The Q-band EPR data are collected in Table XV. No appreciable temperature dependency was seen in either the X- or Q-band spectra for any compound in the range from room temperature to liquid-nitrogen temperature. Each of the compounds showed one somewhat asymmetric derivative in its X-band spectrum at a field of ca. 3200 G and a weak $\Delta M_s = 2$ transition at ca. 1600 G. Signals assignable to singlet-to-triplet transitions were not observed for the eight copper(II) complexes.

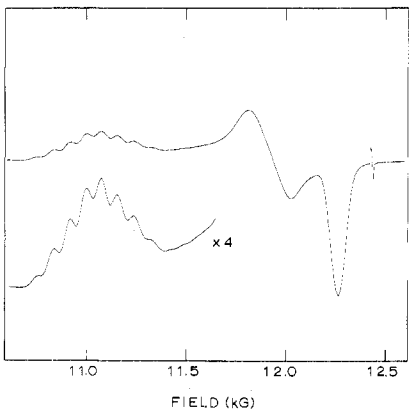

Figure 4. Liquid-nitrogen temperature Q-band EPR spectrum of a powdered sample of $[Cu_2(dien)_2(DHNQ)](BPh_4)_2$.

Copper hyperfine splitting was noted for only one of the compounds run as a pure undoped solid. The Q-band EPR spectrum for a powdered sample of $[Cu_2(dien)_2(DHNQ)](BPh_4)_2$ at liquid-nitrogen temperature is shown in Figure 4. An eight-line copper hyperfine pattern is visible on the parallel signal at $g = 2.251$. The fact that only this compound exhibits such hyperfine splitting led, of course, to the selection of $[Cu_2(dien)_2(DHNQ)](BPh_4)_2$ for single-crystal X-ray structural work. The average interline spacing is ca. 84 G in the eight-line hyperfine pattern.[25] This hyperfine pattern is a clear indication of the presence of a magnetic exchange interaction in $[Cu_2(dien)_2(DHNQ)](BPh_4)_2$ and that the interaction is between the two copper(II) ions in a binuclear complex and is not *inter*molecular in nature. The exchange interaction is greater in magnitude than the copper hyperfine interaction and, therefore, $|J| >$ ca. 0.02 cm^{-1}. Weak *intra*molecular exchange interactions could also be present in the other seven binuclear copper(II) complexes, but, for various reasons, no copper hyperfine pattern was seen in the spectra of the other seven complexes. Apparently, the BPh_4^- anions are at the borderline for providing effective magnetic dilution between the binuclear copper(II) complexes. At this time, however, an intramolecular exchange interaction can only be definitively said to be present in $[Cu_2(dien)_2(DHNQ)](BPh_4)_2$ of all the compounds in this study.

The spectral features seen in the $[Cu_2(dien)_2(DHNQ)](BPh_4)_2$ spectrum (Figure 4) can be analyzed in detail. The eight-line hyperfine pattern results from the overlap of two seven-line patterns, where the spacing between the two seven-line patterns is the consequence of zero-field splitting. The experimental zero-field splitting is found to be $D = 84$ G = 0.0078 cm^{-1}. If the zero-field splitting is dipolar in nature, the maximum value is given by $D_{dd} = (0.65g_{\parallel}^2)/r^3$. The Q-band spectrum gives $g_{\parallel} = 2.251$ and the crystal structure gives a value for the Cu–Cu distance of $r = 8.075$ (3) Å. When these two values are put into the equation, the maximum dipolar zero-field splitting on the $g_{\parallel}$ signal is calculated to be $D_{dd} = 67$ G = 0.0063 cm^{-1}. The relatively small difference is probably due to pseudodipolar zero-field interactions. The X-band spectrum shows a signal centered at $g =$ ca. 2.30 with eight hyperfine lines visible. Finally, the pattern of g values with $g_{\parallel} = 2.251$ and a split $g_{\perp}$ signal ($g = 2.096$ and 2.032)

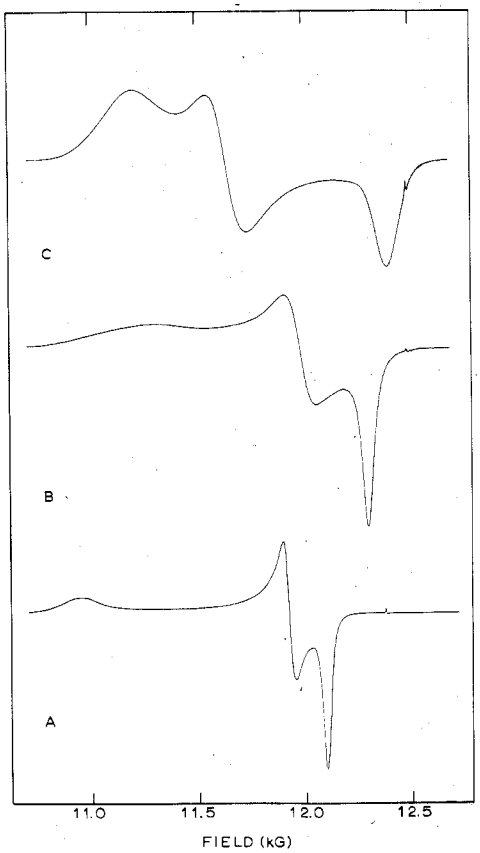

Figure 5. Q-band EPR spectra for powdered samples of (A) $[Cu_2(dien)_2(QUIN)](BPh_4)_2$, (B) $[Cu_2(Me_5dien)_2(QUIN)](BPh_4)_2$, and (C) $[Cu_2(dpt)_2(QUIN)](BPh_4)_2$.

indicates a distorted square-pyramidal copper(II) coordination geometry as was found in the crystal structure.

The Q-band EPR spectra for the series $[Cu_2(dien)_2(QUIN)](BPh_4)_2$, $[Cu_2(Me_5dien)_2(QUIN)](BPh_4)_2$, and $[Cu_2(dpt)_2(QUIN)](BPh_4)_2$ (powdered solids at liquid-nitrogen temperature) are shown in Figure 5. As can be seen, each spectrum is rhombic. There is a change in the pattern from one compound to another and this indicates a change in the local copper(II) coordination geometry. Tracing A illustrates the spectrum for the dien–QUIN compound which is very similar, except for the hyperfine pattern, to the spectrum observed for the dien–DHNQ compound, see Figure 4. This pattern indicates a distorted square-pyramidal copper(II) coordination geometry.[26] The absence of copper hyperfine splitting in the case of the QUIN compound could result from weak intermolecular exchange interactions and resultant electron delocalization precipitated by the extra fused ring of the quinizarin bridge compared to the dihydroxynaphthoquinone bridge.

Tracing B in Figure 5 illustrates the spectrum for the Me_5dien–QUIN compound. This pattern is probably characteristic of a copper(II) geometry that is intermediate between square pyramidal and trigonal bipyramidal. The highest field signal has $g = 2.031$ which could point to some degree of trigonal-bipyramidal geometry. On the other hand, the lowest field signal at $g = 2.225$ is the broadest and appears to be an envelope of exchange-broadened copper hyperfine, which would be characteristic of the $g_{\|}$ signal of a square-pyramidal geometry.

Tracing C in Figure 5 indicates that the copper(II) coordination geometry in the dpt–QUIN compound is that of a distorted trigonal bipyramid[26] where $g_{\|} = 2.021$ and the $g_{\perp}$ signal is split into two features at lower field. It is important to note that no appreciable magnetic exchange interaction is seen for any of these copper(II) complexes in spite of the fact that the coordination geometry varies from square pyramidal to trigonal bipyramidal.

Table XVI. Magnetic Exchange Parameters and Intramolecular Ni–Ni Distances in the Series $[Ni_2(tren)_2(bridge)](BPh_4)_2$[a]

compound	J, cm^{-1}	Ni–Ni, Å
$[Ni_2(tren)_2(Ox)](BPh_4)_2$	-16[b]	5.4[c]
$[Ni_2(macro)_2(Sq)](ClO_4)_2$[d]	-0.4[b]	6.9[e]
$[Ni_2(tren)_2(DHBQ)](BPh_4)_2$	-1.1[f]	7.9[f]
$[Ni_2(tren)_2(DHNQ)](BPh_4)_2$	>-0.1[g]	8.1[h]

[a] The various bridges are the following: Ox, oxalate, $C_2O_4^{2-}$; Sq, squarate, $C_4O_4^{2-}$; DHBQ, dianion of 2,5-dihydroxy-1,4-benzoquinone, $C_6O_4^{2-}$; DHNQ, dianion of 5,8-dihydroxy-1,4-naphthoquinone, $C_{10}O_4^{2-}$. [b] Reference 12 and D. M. Duggan, Ph.D. Thesis, University of Illinois, 1974. [c] Taken from the structure of $[Ni_2(en)_4(Ox)](NO_3)_2$.[20] [d] Reference 12, where macro is 2,4,4,9,9,11-hexamethyl-1,5,8,12-tetraazacyclotetradecane. Attempts to prepare $[Ni_2(tren)_2(Sq)](BPh_4)_2$ were not successful. [e] Estimated. [f] Reference 11. [g] This work. [h] Taken from the Cu–Cu distance in $[Cu_2(dien)_2(DHNQ)](BPh_4)_2$, this work.

An examination of Table XV shows that the same variation in EPR signals and, therefore, copper(II) coordination geometries is found for $[Cu_2(triamine)_2(DHNQ)](BPh_4)_2$, where the triamine is either dien, Me_5dien, or dpt, as was found for the analogous QUIN series. Because the two bridges $DHNQ^{2-}$ and $QUIN^{2-}$ are expected to be structurally very similar, it is reasonable that the local copper(II) geometries are essentially the same in analogous compounds and that changing the triamine ligand leads to the same changes in geometries.

Magnetic Exchange Mechanism. The present study has shown that binuclear copper(II) and nickel(II) complexes bridged by the dianions of 5,8-dihydroxy-1,4-naphthoquinone, 1,4-dihydroxy-9,10-anthraquinone, and 1,5-dihydroxy-9,10-anthraquinone do not show any signs of a magnetic exchange interaction in magnetic susceptibility data taken down to 4.2 K. Because the coordination geometry about a copper(II) ion is so flexible and an exchange interaction depends on the exact ground state,[18] it will be the objective of this section to qualitatively explain the variation in exchange parameter, J, in the series $[Ni_2(tren)_2(bridge)](BPh_4)_2$, where the bridge is variously oxalate ($C_2O_4^{2-}$), squarate ($C_4O_4^{2-}$), the dianion of 2,5-dihydroxy-1,4-benzoquinone (DHBQ), and the dianion of 5,8-dihydroxy-1,4-naphthoquinone. The exchange parameters and estimated Ni–Ni distances are given in Table XVI for this series. It is noted that in the case of the squarate compound, it did not prove possible to prepare a sample of $[Ni_2(tren)_2(C_4O_4)](BPh_4)_2$. However, the compound $[Ni_2(macro)_2(C_4O_4)](ClO_4)_2$ has been shown[12] to have $J = -0.4$ cm^{-1}. macro is the tetraamine macrocyclic ligand 2,4,4,9,9,11-hexamethyl-1,5,8,12-tetraazacyclotetradecane and it is known from other studies[12] that a variation in the backside tetraamine ligand does not appreciably affect the J value in a binuclear nickel(II) complex.

The most obvious conclusion that can be made from the data in Table XVI is that the magnitude of the antiferromagnetic exchange interaction is not simply dependent on the Ni–Ni distance. Thus, the oxalate compound with Ni–Ni = ca. 5.4 Å shows the strongest such interaction with $J = -16$ cm^{-1}. Increasing the Ni–Ni distance by 1.5 Å with the squarate compound leads to a reduction in the magnitude of the interaction to $J = -0.4$ cm^{-1}. An even further increase in the Ni–Ni distance by another 1.0 Å in the $DHBQ^{2-}$-bridged complex does not, however, lead to a further reduction in the magnitude of the antiferromagnetic interaction, but instead, there is an increase to give $J = -1.1$ cm^{-1}. And finally, in the present study, it was found that a relatively small change in the Ni–Ni distance from 7.9 Å for the $DHBQ^{2-}$ complex to ca. 8.1 Å for the $DHNQ^{2-}$-bridged system reduces the level of interaction by another order of magnitude to where J is

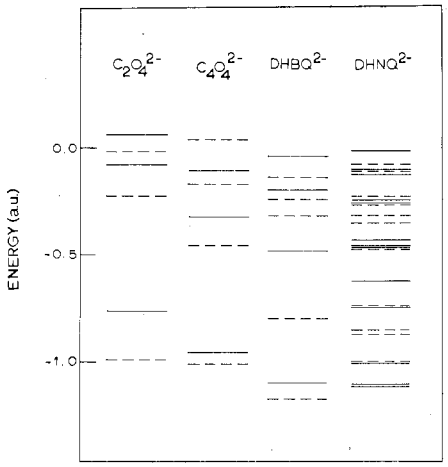

Figure 6. CNDO/2 molecular orbital energies for a series of dianionic bridges, where $C_2O_4^{2-}$ is oxalate, $C_4O_4^{2-}$ is squarate, DHBQ^{2-} is the dianion of 2,5-dihydroxy-1,4-benzoquinone, and DHNQ^{2-} is the dianion of 5,8-dihydroxy-1,4-naphthoquinone. The first three have D_{2h} symmetry and the solid lines are for b_{1g} symmetry orbitals, whereas the dashed lines are for b_{2u} symmetry orbitals. The symmetry of DHNQ^{2-} is C_{2h} and, in this case, the solid lines are for a_g symmetry orbitals and the dashed lines are for b_u symmetry orbitals.

more positive than ca. -0.05 cm^{-1}. The magnitude of the antiferromagnetic interaction is not a function of the Ni–Ni distance, but reflects the viability of the bridge to interact with the metal orbitals in which the unpaired electrons reside.

In a previous paper[11] the variation in exchange parameter in going from oxalate to squarate to 2,5-dihydroxy-1,4-benzoquinone dianion bridge in $[Ni_2(tren)_2(bridge)](BPh_4)_2$ was rationalized by recourse to CNDO/2 molecular orbital calculations for the three bridging dianions. The conclusions of this paper can be briefly reviewed. At the outset, however, it should be pointed out that the caption for Figure 8 (energy level diagram) in that previous paper did have an inadvertent error: the solid lines in the figure should have been labeled as pertaining to b_{1g} symmetry molecular orbitals. Figure 6 summarizes again the results from the previous paper and allows a comparison with the present results. In Figure 6 are plotted the energies of the filled CNDO/2 molecular orbitals of oxalate, squarate, and DHBQ^{2-} that are of either b_{1g} (solid lines) or b_{2u} (dashed lines) symmetry (D_{2h} point group). In these binuclear nickel(II) complexes, each nickel(II) ion has two unpaired electrons, one in a $d_{x^2-y^2}$ orbital that is coplanar with the bridge plane and the other in a d_{z^2} orbital which is not interacting appreciably with the bridge orbitals. A bridging moiety is most effective in supporting an *antiferromagnetic* exchange interaction between two nickel(II) ions if the bridge has available molecular orbitals that can interact with the "bonding" combination of two metal $d_{x^2-y^2}$ orbitals.[11,27] In the D_{2h} point group appropriate for oxalate, squarate, and DHBQ^{2-}, bridge orbitals of b_{1g} symmetry provide the main pathways for an antiferromagnetic interaction. The previous CNDO/2 calculations, as summarized in Figure 6, showed that the marked reduction in interaction in going from oxalate to squarate is a consequence of the fact that the highest energy filled b_{1g} orbital of the squarate is at considerably lower energy (more stable) than the highest b_{1g} orbital of the oxalate dianion. (The filled metal 3d orbitals are at even higher energies than the bridge orbitals.) The interaction observed for the DHBQ^{2-} compound is greater than that observed for the squarate compound because the DHBQ^{2-} bridge has a higher energy b_{1g} orbital; the DHBQ^{2-} bridge also has more filled orbitals of b_{1g} symmetry. Thus, just by comparing the energies (and overlap characteristics) of the highest energy b_{1g} orbitals for oxalate, squarate, and DHBQ^{2-} it is possible to qualitatively rationalize the observed trend in antiferromagnetic interaction.

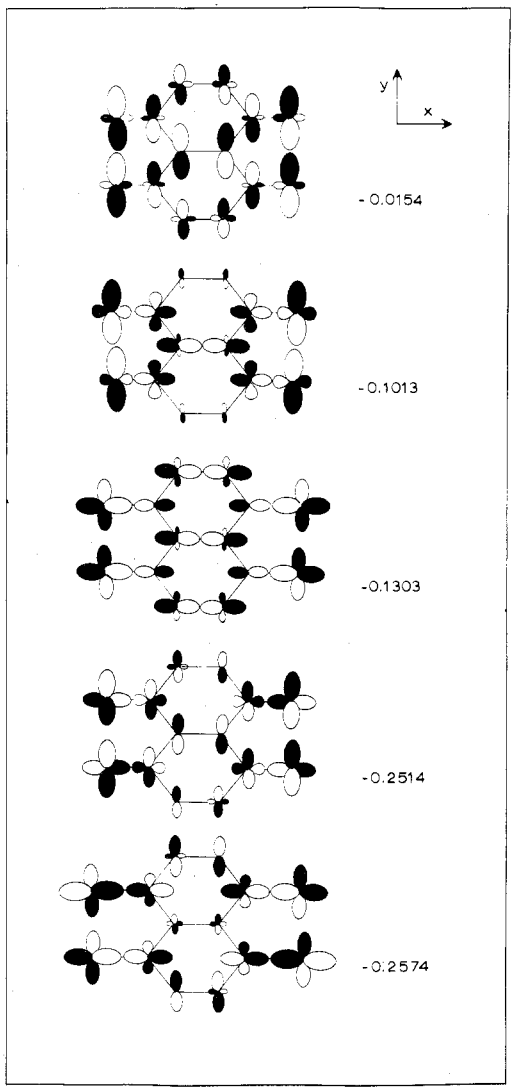

Figure 7. Sketches of the five highest occupied a_g symmetry molecular orbitals of DHNQ^{2-}. Energies are given in atomic units.

In the present study, then, it is important to rationalize why the weakest antiferromagetic interaction with $J >$ ca. -0.05 cm^{-1} is found for $[Ni_2(tren)_2(DHNQ)](BPh_4)_2$. CNDO/2 molecular orbital calculations were carried out for DHNQ^{2-} employing the molecular dimensions of the DHNQ^{2-} moiety found in the structure of $[Cu_2(dien)_2(DHNQ)](BPh_4)_2$. The DHNQ^{2-} unit in this compound has C_{2h} symmetry; the bonding combination of two nickel(II) $d_{x^2-y^2}$ orbitals is of a_g symmetry. (The antibonding combination of two $d_{x^2-y^2}$ orbitals is of b_u symmetry.) The energies of the filled DHNQ^{2-} orbitals of either a_g (solid lines) or b_u (dashed lines) symmetry are indicated in Figure 6. The filled a_g symmetry orbitals of DHNQ^{2-} would be expected to be most effective in propagating an antiferromagnetic interaction between the two nickel(II) ions. There are 13 filled a_g symmetry orbitals for DHNQ^{2-}. As can be seen in Figure 6, the highest energy a_g orbital for DHNQ^{2-} is at higher energy than the corresponding orbital for DHBQ^{2-}. On the basis of only orbital energies, DHNQ^{2-} might be expected to support a greater antiferromagnetic interaction than the DHBQ^{2-} bridge. Figure 7 illustrates the composition of the five highest energy a_g orbitals of DHNQ^{2-} and shows why this is not the case.

The a_g symmetry DHNQ^{2-} orbital at an energy of -0.0154 au will not propagate an antiferromagnetic interaction between two nickel $d_{x^2-y^2}$ unpaired electrons because this orbital has

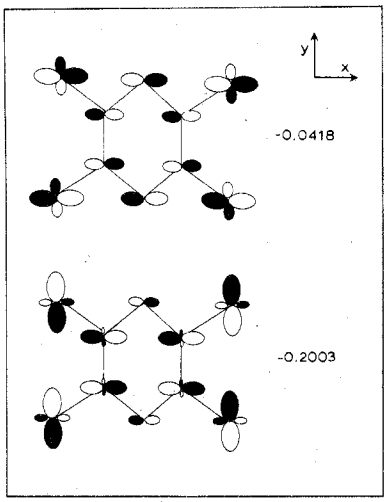

Figure 8. Sketches of the two highest occupied b_{1g} symmetry molecular orbitals of $DHBQ^{2-}$. Energies are given in atomic units.

a node which interrupts the interaction between the two metal unpaired electrons, one at each nickel(II) ion. A node is also present in the a_g symmetry orbital at an energy of −0.2514 au. The $DHNQ^{2-}$ orbital at −0.1013 au does not have such a node and can be seen to have an effective overlap between $2p_x$ orbitals located at carbon atoms C(3) and C(3′). However, this orbital is also not effective at propagating an antiferromagnetic interaction between the two nickel $d_{x^2-y^2}$ unpaired electrons because the $d_{x^2-y^2}$ orbitals would not overlap appreciably with this second highest a_g orbital. Oxygen $2p_y$ orbitals are predominantly employed at the oxygen centers and they are not phased properly to interact with a nickel(II) $d_{x^2-y^2}$ orbital. In other words, a localized orbital view of this orbital presents p-type hybrids at each oxygen atom that do not effectively overlap with the metal $d_{x^2-y^2}$ orbitals. The a_g orbital at −0.1303 au also has this same problem and can be discounted as an effective pathway for an antiferromagnetic interaction. And, finally, the $DHNQ^{2-}$ a_g orbital at −0.2574 au also does not seem to be structured such that it would support such an interaction. This orbital would overlap somewhat with the nickel(II) $d_{x^2-y^2}$ orbitals; however, there is little effective overlap at the three central C–C interactions of the $DHNQ^{2-}$. There is but a weak overlap at C(3)–C(3′) resulting from a minor contribution of properly phased C(3) and C(3′) $2p_x$ orbitals.

For comparison, Figure 8 shows two of the highest energy b_{1g} symmetry (D_{2h} point group; correlates with a_g symmetry in the C_{2h} point group) orbitals of $DHBQ^{2-}$. It can be seen that these two orbitals do offer effective pathways for an antiferromagnetic interaction between two nickel(II) $d_{x^2-y^2}$ unpaired electrons. Both orbitals exhibit effective overlap through the bridge and have atomic orbitals at the oxygen atoms that are phased properly to interact with the metal $d_{x^2-y^2}$ orbitals. This explains why the $DHBQ^{2-}$ bridge is so much more effective in propagating an antiferromagnetic interaction compared to the $DHNQ^{2-}$ bridge; this is in spite of the fact that the metal–metal distance is only 0.2 Å greater in the $DHNQ^{2-}$ bridged complex.

Acknowledgment. C.G.P. wishes to thank Mr. R. C. Haltiwanger for help with data collection and the University of Colorado Computing Center for a generous allocation of computational time. D.N.H. is grateful for support from National Institutes of Health Grant HL 13652.

Registry No. $[Cu_2(dien)_2(DHNQ)](BPh_4)_2$, 67904-68-1; $[Cu_2(Me_5dien)_2(DHNQ)](BPh_4)_2$, 67872-53-1; $[Cu_2(dpt)_2(DHNQ)](BPh_4)_2$, 67872-55-3; $[Cu_2(dien)_2(DHAQ)](BPh_4)_2$, 67872-57-5; $[Cu_2(dpt)_2(DHAQ)](BPh_4)_2$, 67904-70-5; $[Cu_2(dien)_2(QUIN)](BPh_4)_2$, 67904-72-7; $[Cu_2(Me_5dien)_2(QUIN)](BPh_4)_2$, 67872-59-7; $[Cu_2(dpt)_2(QUIN)](BPh_4)_2$, 67872-61-1; $[Ni_2(tren)_2(DHNQ)](BPh_4)_2$, 67872-63-3; $[Ni_2(tren)_2(QUIN)](BPh_4)_2$, 67938-37-8; 1,5-dinitronaphthalene, 605-71-0.

Supplementary Material Available: Tables I (analytical data) and VII–XIV (experimental and calculated magnetic susceptibility data) and final values of $10F_o$ and $10F_c$ for $[Cu_2(dien)_2(DHNQ)](BPh_4)_2$ (19 pages). Ordering information is given on any current masthead page.

References and Notes

(1) Part 17: T. R. Felthouse and D. N. Hendrickson, *Inorg. Chem.*, **17**, 2636 (1978).
(2) University of Colorado.
(3) University of Illinois.
(4) Camille and Henry Dreyfus Fellow, 1972–1977; A. P. Sloan Foundation Fellow, 1976–1978.
(5) R. E. Moore and P. J. Scheuer, *J. Org. Chem.*, **31**, 3272 (1966).
(6) (a) M. Schnitzer and S. U. Khan, "Humic Substances in the Environment", Marcel Dekker, New York, N.Y., 1972; (b) R. H. Thompson, "Naturally Occurring Quinones", 2nd ed, Academic Press, New York, N.Y., 1971; (c) S. Patai, Ed., "The Chemistry of the Quinonoid Compounds", Parts 1 and 2, Wiley, New York, N.Y., 1974.
(7) C. G. deLima and A. DuFresne, *Inorg. Nucl. Chem. Lett.*, **7**, 843 (1971).
(8) C. G. deLima and A. DuFresne, *Inorg. Nucl. Chem. Lett.*, **35**, 789 (1973).
(9) M. S. Masoud, T. M. Salem, and M. H. Amin, *Rocz. Chem. Ann. Soc. Chim. Pol.*, **49**, 1981 (1975).
(10) S. B. Padhyé, C. R. Joshi, and B. A. Kulkarni, *J. Inorg. Nucl. Chem.*, **39**, 1289 (1977).
(11) C. G. Pierpont, L. C. Francesconi, and D. N. Hendrickson, *Inorg. Chem.*, **16**, 2367 (1977).
(12) D. M. Duggan, E. K. Barefield, and D. N. Hendrickson, *Inorg. Chem.*, **12**, 985 (1973).
(13) Supplementary material.
(14) C. Kuroda and M. Wada, *Sci. Pop. Inst. Phys. Chem. Res. (Tokyo)*, **34**, 1740 (1938).
(15) H. F. Holtzclaw, Jr., and H. D. Coble, *J. Inorg. Nucl. Chem.*, **36**, 1049 (1974).
(16) R. S. Bottei and P. L. Gerace, *J. Inorg. Nucl. Chem.*, **23**, 245 (1961).
(17) M. Kirszenbaum, *J. Chim. Phys.*, **74**, 317 (1977).
(18) T. R. Felthouse, E. J. Laskowski, and D. N. Hendrickson, *Inorg. Chem.*, **16**, 1077 (1977).
(19) C. G. Pierpont, *Inorg. Chem.*, **16**, 636 (1977).
(20) N. F. Curtis, I. R. N. McCormick, and T. N. Waters, *J. Chem. Soc., Dalton Trans.*, 1537 (1973).
(21) P. D. Cradwick and D. Hall, *Acta Crystallogr., Sect. B*, **27**, 1990 (1971).
(22) J. G. Rodriguez, F. H. Cano, and S. Garcia-Blanco, *Acta Crystallogr., Sect. B*, **33**, 491 (1977).
(23) G. R. Hall, D. M. Duggan, and D. N. Hendrickson, *Inorg. Chem.*, **14**, 1956 (1975).
(24) D. M. Duggan and D. N. Hendrickson, *Inorg. Chem.*, **13**, 2929 (1974).
(25) The parallel copper hyperfine splitting for a binuclear complex should be half that (150–220 G) found for an analogous monomeric complex: see C. P. Slichter, *Phys. Rev.*, **99**, 479 (1955).
(26) B. J. Hathaway and D. E. Billing, *Coord. Chem. Rev.*, **5**, 143 (1970).
(27) P. J. Hay, J. C. Thibeault, and R. Hoffmann, *J. Am. Chem. Soc.*, **97**, 4884 (1975).